Matrix stiffness and cluster size collectively regulate dormancy versus proliferation in brain metastatic breast cancer cell clusters

Journal:	*Biomaterials Science*
Manuscript ID	BM-ART-06-2020-000969.R1
Article Type:	Paper
Date Submitted by the Author:	07-Sep-2020
Complete List of Authors:	Kondapaneni, Raghu Vamsi; The University of Alabama, Chemical and Biological Engineering Rao, Shreyas; The University of Alabama, Chemical and Biological Engineering

SCHOLARONE™
Manuscripts

Matrix stiffness and cluster size collectively regulate dormancy versus proliferation in brain metastatic breast cancer cell clusters

Raghu Vamsi Kondapaneni[1] and Shreyas S. Rao [1] *

[1]Department of Chemical and Biological Engineering, The University of Alabama, Tuscaloosa, Alabama 35487, United States

* Corresponding author

Shreyas S. Rao, Ph.D.

Department of Chemical and Biological Engineering

The University of Alabama

Tuscaloosa, AL, 35487-0203, USA

Office: SEC 3453

Phone: (205) 348-6564

Fax: (205) 348-7558

Email: srao3@eng.ua.edu

Abstract

Breast cancer cells can metastasize either as single cells or as clusters to distant organs from the primary tumor site. Cell clusters have been shown to possess higher metastatic potential compared to single cells. The organ microenvironment is critical in regulating the ultimate phenotype, specifically, the dormant versus proliferative phenotype, of these clusters. In the context of breast cancer brain metastasis (BCBM), tumor cell cluster-organ microenvironment interactions are not well understood, in part, due to the lack of suitable biomimetic *in vitro* models. To address this need, herein, we report a biomaterial-based model, utilizing hyaluronic acid (HA) hydrogels with varying stiffnesses to mimic the brain microenvironment. Cell spheroids were used to mimic cell clusters. Using 100 – 10,000 MDA-MB-231Br BCBM cells, six different sizes of cell spheroids were prepared to study the impact of cluster size on dormancy. On soft HA hydrogels (~0.4 kPa), irrespective of spheroid size, all the cell spheroids attained a dormant phenotype, whereas on stiff HA hydrogels (~4.5 kPa), size dependent switch between dormant versus proliferative phenotype was noted (i.e., Proliferative phenotype $\geq$ 5000 cells cluster < Dormant phenotype) as tested via EdU and Ki67 staining. Further, we demonstrated that the matrix stiffness driven dormancy was reversible. Such biomaterial systems provide useful tools to probe cell cluster-matrix interactions in BCBM.

Keywords: Dormancy, Cell clusters, Breast cancer brain metastasis, Extracellular matrix, stiffness, Hyaluronic acid.

1. Introduction

The ability of breast cancer cells to metastasize to distant organs accounts for ~90% of breast cancer related mortalities[1, 2]. Specifically, breast cancer cells are known to metastasize to the lungs, brain, liver, bone, and lymph nodes[3]. In some cases, metastasis may occur even before the detection of the primary tumor[4]. Furthermore, recent studies have demonstrated that collective cell migration (i.e., as a cluster of cells) and dissemination possesses a significantly higher probability of evolving into metastasis, compared to single cell migration and invasion[5-7]. However, the mechanisms regulating the colonization of organ sites by metastatic tumor cell clusters are not well understood.

Accumulating evidence suggests that there is a latency period between dissemination and metastatic outgrowth [8, 9]. During this period, tumor cells may attain a dormant state, where the cells are either growth-arrested (cellular dormancy) or the cell growth is balanced by apoptosis occurring within the tumor (mass dormancy)[9]. Disseminated tumor cells are capable of developing metastasis, even after sustaining an extended period of dormancy for decades[8-10]. Despite the progress in developing therapeutic strategies, the 5-year survival rate for patients with breast cancer metastasis in the United States is only 26%[11]. Breast Cancer Brain Metastasis (BCBM) is the most aggressive with a median survival period of only 4-16[12] months. This is mostly attributed to poor prognosis and, in part, to the lack of understanding of the underlying mechanisms involved in tumor relapse at the metastatic site. This is further hampered by the lack of relevant experimental model systems to study and elucidate the underlying mechanisms involved in the reawakening of dormant BCBM cells.

It is now well recognized that the tumor microenvironment plays a significant role in modulating the dormant phenotype of disseminated tumor cells [8, 9, 13-15], consistent with the "seed and soil"

theory proposed in 1889[16]. Specifically, the extracellular matrix (ECM) is critical in determining the fate of disseminated tumor cells [17, 18]. In order to develop an *in vitro* model to study tumor dormancy, it is imperative to incorporate the ECM to capture the cell – ECM interactions. To this end, many studies have utilized various natural, synthetic, and semi-synthetic biomaterials to mimic the ECM, such as basement membrane matrix (Matrigel)[19-21], collagen[22, 23], fibrin gel[24], hyaluronic acid (HA)[25], polyethylene glycol (PEG)[26], polyacrylamide[27] and Amikagel[28] to study the regulation of dormancy in the context of the primary tumor setting.

Few studies have been reported to investigate tumor dormancy in the metastatic setting. For example, dormancy in bone metastatic breast cancer cells has been studied by utilizing biomaterial-based[29] and bioreactor-based models[30], whereas microfluidic-based co-culture models have been used to study dormancy in liver metastatic breast cancer cells[31, 32]. More recently, our group reported a HA hydrogel based platform to investigate dormancy in BCBM cells at the single cell level[12]. These models provide insightful information about the mechanisms regulating tumor dormancy at a single cell level. However, to the best of our knowledge, there are no reported *in vitro* models investigating dormancy in BCBM cell clusters.

Herein, we report an *in vitro* biomaterial-based model to study microenvironmental regulation of dormancy in BCBM cell clusters. We utilized HA hydrogels to mimic the native brain ECM, as HA is one of the most abundant components of the brain ECM and is highly secreted in brain metastatic lesions[33, 34]. We prepared two versions of the HA hydrogels, namely soft (i.e., 0.4 kPa) and stiff (i.e., 4.5 kPa) HA hydrogels, which bracketed the native brain stiffness and that reported for brain metastasis[12]. Tumor cell spheroids were employed to mimic cell clusters. To study the effect of cluster size, six different sizes of cell spheroids were prepared by using 100 - 10,000 BCBM cells. Cell spheroids were cultured on top of both the hydrogels to evaluate the effect of

matrix stiffness on dormancy vs. proliferation of cell clusters. Cell spheroids were also cultured in suspension and adherently (i.e., on tissue culture polystyrene (TCPS)) to investigate the effect of culture conditions on cell cluster phenotypes. Finally, we also tested the reversibility of the dormant phenotype in this system.

2. Experimental

2.1. Cell Culture

td-Tomato expressing MDA-MB-231Br, a brain metastatic breast cancer cell line, derived from a triple negative breast cancer cell line MDA-MB-231 was used in this study and was cultured as described previously[12]. Briefly, cells were maintained in Dulbecco's Modified Eagle Medium-high Glucose (DMEM) (Sigma Aldrich) media supplemented with 10% fetal bovine serum (FBS) (VWR Life Science) and 1% Penicillin-Streptomycin (PS) (Gibco) at 37 ^oC and 5% CO_2 environment.

2.2. HA Hydrogel Preparation

Synthesis of hyaluronic acid methacrylate (HAMA) was performed using previously established procedures[12, 35, 36]. Briefly, a 1 wt% solution of Sodium Hyaluronate (66-90 kDa; Lifecore Biomedical) was prepared in deionized water overnight and subjected to ~18 fold molar excess of methacrylic anhydride (Sigma Aldrich) at 4 ^oC , by maintaining the pH between 8-10 using 5M NaOH. A fivefold volumetric excess of cold acetone was added to the reaction mixture to extract HAMA, which was then flash frozen and lyophilized overnight. Proton nuclear magnetic resonance (^{1}H-NMR) was utilized to measure the degree of methacrylation and in this study HAMA with ~85% degree of methacrylation was used. Next, a gel precursor solution was prepared using 5 wt% HAMA solution in DMEM and dithiothreitol (DTT) (Sigma Aldrich), and 80 µL of this solution was added to each well of a 96-well plate and incubated overnight for

gelation. Different concentrations of DTT were used to obtain hydrogels with varying stiffness i.e., 10 mM for soft hydrogel (~0.4 kPa) and 40 mM for stiff hydrogel (~4.5 kPa), respectively, as determined via compression testing using a RSA-G2 solid analyzer (TA Instruments)[12, 36]. To enhance cell adhesion, surfaces of both soft and stiff HA hydrogel was consistently functionalized with an integrin binding peptide (RGD) (Anaspec) as reported previously[36].

2.3. Tumor cell spheroid construction

Cell spheroids were prepared utilizing a previously established protocol [37]. Briefly, 20 mg/ml of Poly(2-hydroxyethyl methacrylate) (p-HEMA) (Sigma Aldrich) solution was prepared by dissolving 500 mg in 25 mL of 95% ethanol for 3 h. Each well of a 96 well round bottom plate (Thermo Fisher Scientific) was coated using ~30 µL of p-HEMA solution to create an ultralow attachment surface for cells, followed by drying the plate overnight in a laminar hood. Next, cell dilutions were prepared based on the cell count needed to prepare spheroids. 100 µL of cell suspension containing the required cell count of MDA-MB-231Br cells was added to the wells of a p-HEMA coated 96 well round bottom plate and the plate was centrifuged at ~1000g for 10 min. After centrifugation, 2.5% of growth factor reduced Matrigel (Corning) was added to wells on v/v basis and the plate was incubated overnight. On the following day, cell spheroids were collected using a 200 µL pipette tip with the tip removed to minimize spheroid disintegration and subsequently cultured on top of soft or stiff HA hydrogels or as a suspension culture on p-HEMA coated flat 96-well plate or as adherent culture on TCPS.

2.4. Optical imaging and cell spheroid area measurements

Cell spheroids cultured in different culture conditions were monitored daily using an Olympus IX83 microscope with a spinning confocal disc attachment. Both bright field and fluorescent images of cell spheroids were captured throughout the culture period to track their growth.

Specifically, day 0 images were taken within half hour post transfer of cell spheroids. Image-J software was utilized to measure the cell spheroid area (cross sectional area of spheroid + spread area of cells (in case cells were migrating from spheroid)) as described earlier[38, 39]. Briefly, the boundary of the cell spheroids was manually selected and if migration was observed from spheroid, their boundaries were also considered to calculate the spheroid areas.

2.5. Dissociation of cell spheroids

For quantification at the single cell level, cell spheroids were dissociated into single cells before staining for various markers. Dissociation of cell spheroids into single cells was performed by adapting the procedure described previously[40]. Briefly, cell spheroids were collected on day 7 into an eppendorf tube and the media was removed, and the spheroids were washed twice with 300 µL of 1X phosphate buffer saline (PBS) (Gibco). Next, 300 µL of Accutase (Corning) was added to the spheroids and incubated for ~5 min at 37 °C. After 5 min of incubation, spheroids were resuspended in Accutase using a 200 µL pipette tip to mechanically disintegrate the spheroids for another ~5 min followed by an additional incubation of ~5 min. This cycle was repeated for ~40 min and the eppendorf tubes were centrifuged for allowing the cells to settle to the bottom. The single cells were then washed twice with PBS and transferred to a 96 well plate for staining protocols.

2.6. 5-Ethynyl-2´-deoxyuridine (EdU) cell proliferation assay

Proliferation of cell spheroids in various culture conditions for a period of 7 days was measured by incorporating EdU (Click-iT® EdU microplate assay kit (Invitrogen- C10214)) into the cell DNA as described in previous studies[12, 38]. Briefly, on day 7, media in each well was replaced with 10 µM EdU containing media and incubated overnight. The media was then removed and the spheroids were dissociated into single cells and transferred into a 96 well plate and fixed for

~5 min by adding 50 µL of click-iT® EdU fixative. Next, 50 µL of the reaction cocktail prepared as per manufacturer's protocol was added to the wells and incubated for 25 min in the dark at room temperature. After incubation, the plate was centrifuged at 1000g for 1 min, followed by washing with PBS twice. Cells were then counterstained with DAPI (Invitrogen) for 5 min in the dark at room temperature. An Olympus IX83 microscope with a spinning confocal disc attachment was used for fluorescence microscopy. Exposure time and gain settings were maintained constant for all the conditions. Multi point tool in ImageJ software was utilized to quantify %EdU positive cells, as described previously[12].

2.7. Immunofluorescence staining

On day 7, cell spheroids cultured in various culture conditions were collected and dissociated into single cells and transferred into a 96 well plate and washed with 100 µL of PBS twice. Next, the cells were fixed at room temperature for 20 min by adding 100 µL of 4% paraformaldehyde, permeabilized in the presence of 0.25% TritonX-100 in 1X PBS for 15 min at room temperature and blocked by adding 5% bovine serum albumin (BSA) in 1X PBS for 30 minutes at 4 °C. Between each step, cells were washed with PBS and before aspirating any solution, the plate was centrifuged at 1000g for 1 min. Cells were then stained for Ki67 protein (ab15580, Abcam) (marker for cellular proliferation), Cleaved caspase-3 (Asp175, Cell Signaling Technology), Vimentin (SC-6260, Santa Cruz Biotechnology), or E-cadherin (SC-21791, Santa Cruz Biotechnology).

Cells were incubated overnight at 4 °C with 100 µL of primary antibody dilutions (1:150 for Ki-67, 1:200 for Vimentin, E-cadherin, and Cleaved caspase-3, respectively,) in 1X PBS. On the following day, cells were washed twice with 1X PBS and incubated at 4 °C for 1hr with 100 µL of fluorescently labeled secondary antibody dilutions (1:1000) in 1X PBS. Alexa Fluor 488-

conjugated goat anti-rabbit secondary antibody (A11034, Invitrogen) was used to detect Ki-67 and Cleaved caspase-3. Alexa Fluor 488- conjugated goat anti-mouse secondary antibody (A11001, Invitrogen) was utilized to detect Vimentin and E-Cadherin. Later, the cells were counterstained with DAPI for 5 min at room temperature. An Olympus IX83 microscope with a spinning confocal disc attachment was used for fluorescence microscopy. Exposure time and gain settings were maintained constant for all the conditions. Multi point tool in ImageJ software was utilized to quantify % Ki67 positive , % Vimentin positive, and % Cleaved caspase-3 positive cells, as described previously[12]. Similar protocol was followed for staining cell spheroids. Cell spheroids were also directly stained for F-actin using AlexaFluor-488 labeled phalloidin (A12379, Invitrogen) using a dilution of 1:500.

2.8. Apoptosis assay

In addition to Cleaved caspase-3 staining, Annexin-V apoptosis detection kit (Santa Cruz Biotechnology) was used to detect the % apoptotic cells present in the 10k cells spheroid by following the protocol prescribed by the manufacturer. Briefly, on day 7, cell spheroids were dissociated into single cells. Single cells were washed twice with PBS and once with 1X assay buffer solution. After washing, 100 μL of 1X assay buffer solution and ~2.5 μL of FITC-conjugated Annexin-V was added to the cells and incubated for 15 min in the dark at room temperature. The cells were then washed twice with PBS. Before aspirating any solution from wells, the plate was centrifuged at 1000g for 1 min, to allow cells to settle to the bottom. An Olympus IX83 microscope with a spinning confocal disc attachment was used for fluorescence microscopy. Exposure time and gain settings were maintained constant for all the conditions. Multi point tool in ImageJ software was utilized to quantify % apoptotic cells, as previously described[12].

2.9. Statistical analysis

All the experiments were performed at least twice with at least 2 replicates for each condition. The data are reported as mean ± standard error unless otherwise mentioned. Statistical analysis was performed using JMP Pro software. Student's t-test or ANOVA followed by Tukey's HSD post-hoc analysis was performed to compare samples depending on the number of available data sets. Statistically significant difference between the data sets was noted for p-value less than 0.05.

3. Results and discussion

In this study, we report an *in vitro* biomaterial based-model, to investigate the impact of ECM stiffness and cell cluster size on the dormant vs. proliferative status of brain metastatic breast cancer cell clusters by utilizing various sizes of MDA-MB-231Br cell spheroids and HA hydrogels with varying stiffness. The impact of ECM stiffness on the behavior of tumor cells at the single cell level has been extensively studied in the context of a primary tumor setting[11, 19, 20, 23-27, 41], however, relatively few studies have been reported in the metastatic setting [12, 29, 36]. Herein, for the first time, we studied the influence of ECM stiffness on BCBM cell clusters, as they are known to possess higher metastatic potential. Further, cell-matrix interactions involved in establishing BCBM are not well understood. To this end, we elucidated the effect of various culture conditions on BCBM cell spheroids by culturing them as suspension and adherent cultures in addition to culture on ECM mimicking HA hydrogels.

3.1. Effect of culture conditions and cell spheroid size on the phenotype of BCBM cell spheroids

Despite the fact that tumor cell clusters possess higher metastatic potential compared to single cells, the interaction between tumor cell clusters and the brain microenvironment is not well

10

understood. Here, a soft (0.4 kPa) and stiff (4.5 kPa) HA hydrogel was formulated to simulate

the ECM stiffness range of the native brain (0.2 -1 kPa[42]) and that noted for metastatic brain

malignancy (3.7 kPa[43]). HA hydrogels were formed by altering the crosslinker concentration

while maintaining similar HA composition. To assess the impact of culture conditions, we

cultured brain metastatic breast cancer cell spheroids in suspension culture, adherent culture on

2D TCPS, as well as on top of the brain ECM mimicking soft (0.4 kPa) and stiff HA (4.5 kPa)

hydrogels. Till date, circulating tumor cell (CTC) clusters composed mostly of 2 to 100 cells

have been detected clinically[44]. Here, to assess the impact of cluster size, cell spheroids were

prepared by employing six different cell densities (i.e., 100, 500, 1k, 2k, 5k and 10k cells),

including the clinically observed 100 cell clusters[44]. Optical imaging showed that uniform and

reproducible cell spheroids were formed within 24 h. These cell spheroids were then transferred

to different culture conditions on the next day and cultured for 7 days. Day 0 bright field and

fluorescent images of cell spheroids (Figure 1a and 1b) show that the cells were compactly

positioned in the spheroids and no scattering of cells was seen even after transfer of the

spheroids. To assess the growth profile of cell spheroids, the area of the cell spheroids was

measured for each day throughout the culture period.

Cell spheroids cultured adherently on 2D TCPS exhibited an enhanced growth profile, where the

cells started to spread on TCPS and in the case of higher cell density spheroids more than half of

the well plate area was covered with cells by the end of day 7 (Figure S1 - S6). As a result, the

day 7 area of all the cell spheroids was at least 10 times greater than the day 0 areas. Thus, only

the area of cell spheroids cultured in suspension, and on soft or stiff HA hydrogel was plotted to

depict the impact of culture conditions on cell spheroids (Figure 1c - 1h). In the case of 100 and

500 cells spheroid, spheroids cultured in suspension displayed a linearly increasing growth trend

as the cell spheroid areas increased from day 0 to day 7 (Figure S1 and S2). Specifically, for the 100 cells spheroid, the day 7 area in suspension culture (37699 ± 8624 μm^2) was ~4 times higher compared to the day 0 area (8828 ± 321 μm^2) and for 500 cells spheroid, the day 7 area in suspension culture was ~7 times greater compared to the day 0 area. In contrast, the areas of 100 and 500 cells spheroid cultured on soft or stiff HA hydrogel remained mostly constant throughout the culture period (Figure 1c and 1d). For 1k and 2k cells spheroid, day 7 spheroid areas for suspension culture was ~7 times higher than the day 0 area and the areas of 1k and 2k cells spheroid cultured on soft HA hydrogel remained largely unchanged from day 0 to day 7. However, a slight increase in area was noted by the end of day 7 for 1k and 2k cells spheroid cultured on the stiff HA hydrogel compared to soft HA hydrogel, although this change was not statistically significant (Figure 1e and 1f).

Even though similar growth profiles were observed for 5k and 10k cell spheroids when cultured in suspension , the fold increase in area over 7 days for 5k (~5 times) and 10k (~2.75 times) cells spheroid were less when compared to 500, 1k and 2k (> 7 times) cells spheroid. When cultured on the soft HA hydrogel, both 5k and 10k cells spheroid exhibited a dormant phenotype, wherein the cell spheroids area was mostly unchanged throughout the culture period. In contrast, on the stiff HA hydrogel, areas of both 5k and 10k cells spheroid increased significantly ($p < 0.05$), as the day 7 area of both the cell spheroids was ~1.8 fold higher compared to soft HA hydrogel (Figure 1g and 1h). Based on area measurements, BCBM cell spheroids exhibited three different phenotypic growth patterns depending on the culture environments. When BCBM cell spheroids were cultured either in suspension or adherent cultures, they exhibited a proliferative phenotype as expected (Figure 1, and S1- S6). When BCBM cell spheroids were cultured on top of soft HA hydrogels, they exhibited a dormant phenotype compared to stiff HA hydrogels (Figure 1).

Further, cell spheroids cultured on top of stiff HA hydrogels displayed a size dependent switch between dormant and proliferative phenotypes (Figure 1).

Interestingly, stiffness mediated cell migration from cell spheroid and micro-colony formation was observed for 10k cells spheroid cultured on the stiff HA hydrogel by day 7. In contrast, when the 10k cells spheroid was cultured on the soft HA hydrogel for a period of 7 days, the spheroid displayed the same morphology throughout the culture time (Figure 2a and 2b). This is consistent with observations made by Ondeck et al., who also recently showed that on stiff methacrylated HA substrates (~5 kPa), cells tends to migrate away from mammary epithelial cell spheroids[45]. In 10k cells spheroid cultured on the stiff HA hydrogel, no cell migration was observed by the end of day 1 (Figure 2c), however, by the end of day 7, we noticed cell migration and micro-colony formation at a significant distance (375 ± 61 μm) from the spheroid (Figure 2d i, ii and 2e). Interestingly, uniform cell migration was not observed throughout the periphery of the spheroid (Figure 2d iii and iv) as seen on 2D TCPS (Figure S6). The maximum area of the micro-colonies formed was similar to that of 100 cells spheroid area; these micro-colonies were as compact as the 100 cells spheroid (Figure 2d v). Taken together, these results indicate that the culture environment, size of the cell clusters, as well as the ECM stiffness play a crucial role in modulating the growth phenotype of cell clusters.

3.2. ECM stiffness driven dormancy and proliferation in BCBM cell spheroids

As the cell spheroids cultured on top of soft or stiff HA hydrogel displayed a dormant vs. proliferative phenotype, we sought to quantify the percentage of proliferating cells present in the cell spheroids. First, we utilized Ki67 staining to detect Ki67 protein, which is used as a marker for cell proliferation, as it is highly expressed during active phases of the cell cycle and absent when the cells are in either a dormant or quiescent phase[46, 47]. Also, many studies have utilized

Ki67 as a marker to study dormancy[12, 22, 29, 31]. We initially stained the cell spheroids cultured on both soft and stiff HA hydrogel directly on day 7 for Ki67. We found that 100, 500, 1k and 2k cells spheroid were largely Ki67 negative (Figure S7-S10) regardless of hydrogel stiffness. However, the 5k and 10k cells spheroids cultured on the stiff HA hydrogel showed some Ki67 positivity indicating the presence of proliferating cells compared to the spheroids cultured on the soft HA hydrogel (Figure S11 and S12). Ki67 staining on cell spheroids directly, qualitatively demonstrated size-dependent dormant vs. proliferative phenotypes on the stiff HA hydrogel and a dormant phenotype on the soft HA hydrogel irrespective of cluster size. Interestingly, micro-colonies formed on stiff HA hydrogel from 10k cells spheroid exhibited Ki67 positivity (Figure S13), however, similar sized 100 cells spheroid were largely Ki67 negative when seeded directly on the stiff HA hydrogel (Figure S7).

To obtain quantitative results, we dissociated the spheroids into single cells and stained them for Ki67. For this analysis, we only utilized 10k cells spheroid, given the dramatic differences in stiffness induced growth characteristics observed in this condition (Figure 1). On day 7, spheroids cultured on top of HA hydrogels were collected and disintegrated into single cells. Ki67 staining of these single cells revealed that spheroids cultured on the stiff HA hydrogel had a 2 fold higher population of Ki67 positive cells compared to the soft HA hydrogel (p<0.05). Specifically, 11.7 ± 1.6 % cells were Ki67 positive when cultured on soft HA hydrogel vs. 27.7 ± 2.3 % on the stiff HA hydrogel (Figure 3). Single cells obtained from 10k cells spheroid cultured in suspension and adherent cultures were also stained for Ki67, indicating 32.6 ± 0.2 % Ki67 positive cells were present in suspension culture, and 52.6 ± 3.8 % Ki67 positive cells in adherent culture (Figure 3). The number of Ki67 positive cells present in 10k cells spheroid

cultured in suspension and adherent cultures was significantly higher when compared to the soft

HA hydrogel ($p < 0.05$).

In addition to Ki67, we also evaluated the % of proliferating cells present in 10k cells spheroid

by incorporating EdU into the newly synthesized DNA. EdU incorporation has been widely used

to measure cell cycle progression (G0/G1 transition) and as a marker to study cancer dormancy[11,

12, 31, 38, 48]. EdU staining was carried out on day 7 for 10k cells spheroid cultured on soft or stiff

HA hydrogel, as well as suspension and adherent cultures. Consistent with Ki67 staining, we

found that % of EdU positive cells present in 10k cells spheroid was significantly higher in the

stiff HA hydrogel compared to the soft HA hydrogel ($p < 0.05$). In particular, 16.4 ± 1.5 % of

EdU positive cells were present in the spheroid cultured on soft HA hydrogel compared to 37.5 ±

0.9 % of EdU positive cells in stiff HA hydrogel (Figure S14). The percentage of EdU positive

cells was significantly higher ($p < 0.05$) in the 10k cells spheroid cultured in suspension (54.9 ±

2.2 %) and adherent cultures (72.8 ± 1.5 %) compared to spheroids cultured on both soft and

stiff HA hydrogel (Figure S14).

To gain mechanistic insights, we performed immunofluorescence staining for Vimentin

(mesenchymal marker), E-Cadherin (epithelial marker) as well as F-actin for the 10k cells

spheroid. We observed an increase in the % of Vimentin-positive cells in 10k cells spheroid on

the stiff HA hydrogel compared to soft HA hydrogel (i.e., 50.8 ± 3.2 % vs. 35.8 ± 3.3%) (Figure

S15 and S16). MDA-MB-231Br cells are derived from MDA-MB-231 (parental cell line) which

exhibit mesenchymal characteristics[49]. Thus, as expected, % of E-Cadherin positive cells were

low (< 2%), and similar on both soft and stiff HA hydrogels (not shown). Migrating cells from

10k cells spheroid on stiff HA hydrogel exhibited a spread morphology at the spheroid periphery

and near the micro colonies (Figure S17 and S18) with a developed actin cytoskeleton, whereas

on soft HA hydrogel no protrusions were seen along the periphery of the 10k cells spheroid (Figure S19). Size dependent dormant vs. proliferative phenotype observed on the stiff HA hydrogel can also be partly attributed to a significant increase ($p < 0.05$) in the percentage of Vimentin positive cells in larger clusters (50.8 ± 3.2 % positive cells in 10k cells spheroid) compared to small clusters (40.6 ± 1.9% positive cells in 500 cells spheroid). Further, % EdU positive cells present in 500 cells spheroid were significantly lower (13.5 ± 1.3 %) compared to 10k cells spheroid (37.5 ± 0.9 %) cultured on stiff HA hydrogels ($p < 0.05$).

Annexin-V as well as Cleaved caspase-3 staining was utilized to quantify apoptotic cells present in the 10k cell spheroids and to examine whether the observed dormant phenotype on the soft HA hydrogel is due to apoptosis. The percentage of apoptotic cells present in 10k cells spheroid cultured on both soft and stiff HA hydrogel were similar and less than 11% (Figure S20 and S21). In particular, the spheroids contained 7.4 ± 1 % Annexin V positive cells in the soft HA hydrogel compared to 5.1 ± 1.1 % in the stiff HA hydrogel. Similarly, 11.2 ± 3.2 % cells stained positive for cleaved caspase-3 in the soft HA hydrogel compared to 7.6 ± 0.9% in stiff HA hydrogel. This result suggests that the dormancy observed on the soft HA hydrogel is primarily due to the impact of ECM stiffness and not due to cell death by apoptosis. In sum, these results demonstrated that spheroids cultured on soft HA hydrogel exhibited a dormant phenotype in comparison to the spheroids cultured on a stiff HA hydrogel that exhibited a size dependent dormant vs. proliferative phenotype. Previously, Singh et al., reported that size dependent migratory characteristics were exhibited by three dimensional breast cancer micro-tumors when cultured on non-adhesive PEG dimethacrylate hydrogel microwells[50, 51]. Herein, we were able to establish a cluster size cut off range for the dormant vs. proliferative phenotype on stiff HA hydrogel for the first time depending on the initial number of cells present in the cluster (i.e.,

Proliferative phenotype $\geq$ 5000 cells < Dormant phenotype). Thus, our data suggests that matrix stiffness and cluster size collectively determine the dormant vs. proliferative phenotype. Based on prior studies[28, 50, 52], it is possible that necrotic cores may be present in 10k cell spheroids (diameter > 400 μm) and may also play a role in the observed phenotype. This would be investigated in future studies.

3.3. Reversibility of ECM stiffness induced dormant phenotype

Reawakening of dormant tumor cells or cell clusters by microenvironmental derived cues has been known to contribute to disease relapse at the metastatic site[9, 11, 13]. Modifications to the ECM, which results in reawakening of single dormant cancer cells have been previously reported *in vitro*[11, 12, 19, 23, 28, 45]. For instance, Barkan et al., demonstrated that incorporation of fibronectin into the ECM (cultrex) drove quiescent single D2.0R breast cancer cells into a proliferative state[19]. A recent study by Pradhan et al., showed that, dormant MDA-MB-231 breast cancer cells can be activated by increasing the adhesiveness of the matrix[11]. In the context of reversing ECM stiffness driven dormancy, Grandhi et al., showed that when dormant 100k T24 (bladder cancer) cells spheroid cultured on ~ 216 kPa Amikagels were transferred to ~36 kPa Amikagels, cell shedding and micro-colony formation was observed[28]. Herein, we tested whether the ECM stiffness induced dormant phenotype was reversible. Specifically, we tested whether the transfer of a dormant spheroid to a stiff HA hydrogel environment would revoke dormancy. For this study, 10k cells spheroid were cultured on a soft HA hydrogel for a period of 7 days, following which, the spheroids were collected and transferred on to a freshly prepared soft or stiff HA hydrogel (Figure 4a) and cultured for an additional 7 days. On the soft HA hydrogel, 10k cells spheroid exhibited a dormant phenotype for the initial 7 days and later when transferred to a new soft HA hydrogel (soft to soft) depicted a similar phenotype till day 14. Upon transfer to a stiff

HA hydrogel (soft to stiff), cell migration from the spheroid was observed (Figure 4b) but, surprisingly, the formation of micro-colonies was not seen during the culture period. Further, the area of the cell spheroids at day 14 for soft to stiff HA hydrogel condition was significantly higher ($p < 0.05$) when compared to soft to soft HA hydrogel condition indicating a dormant-to-proliferative switch (Figure 4c).

These results were further supported by Ki67 staining. In the case of spheroids cultured on soft to stiff HA hydrogel for 14 days, % of Ki67 positive cells were 2 fold higher ($p < 0.05$) when compared to soft to soft HA hydrogel. In particular, 19.2 ± 1.6 % of cells were Ki67 positive in soft to stiff HA hydrogel compared to 9.2 ± 0.8 % in soft to soft HA hydrogel (Figure 5). In addition, we also evaluated whether the dormant spheroids could attain a proliferative phenotype when they were transferred to 2D TCPS (i.e., soft to adherent) culture condition. Herein, 10k cells spheroids were transferred to 2D TCPS after culturing on soft HA hydrogel for 7 days. Transfer of these dormant spheroids to 2D TCPS also triggered the phenotypic switch from dormant to proliferative phenotype, over the course of 7 additional days in culture. Specifically, the area of the cell spheroids cultured in soft to adherent was significantly higher ($p < 0.05$) when compared to soft to soft condition. Additionally, the % of Ki67 positive cells in soft to adherent condition (34 ± 3 %) was ~3.5 times higher compared to soft to soft condition (9.2 ± 0.8 %) (Figure S22). Modulation of the culture environment resulted in cell migration from spheroids similar to observations by Grandhi et al[28], whereas spheroids retained dormant phenotype if cultured in a similar microenvironment (i.e., soft HA hydrogel) (Figure 4, 5 and S22). Taken together, these results indicated that the observed dormant phenotype was, indeed, reversible by modulating the culture environment.

Some limitations of this study that should be taken into consideration are as follows: (i) *In vivo*, CTC clusters may also contain immune cells that can impact the growth of CTC clusters[5, 53] and the future studies should examine the interactions between CTC clusters and immune cells. (ii) Herein, the top-seeded culture was employed (as opposed to encapsulation) to specifically evaluate the impact of matrix stiffness and cluster size and future studies could examine how encapsulation of cell clusters impacts their phenotype. Overall, by utilizing a biomimetic HA hydrogel platform to recapitulate the brain microenvironment, we elucidated metastatic site specific cell cluster - ECM interactions (i.e., ECM stiffness induced dormancy, spheroid size dependent dormant vs. proliferative phenotypes, formation of micro-colonies, and reawakening of dormant cell spheroids) in a single *in vitro* platform.

4. Conclusions

Here, we successfully utilized biomimetic HA hydrogels with variable stiffnesses and six different sizes of cell spheroids to evaluate the impact of ECM stiffness and cluster size on the dormant versus proliferative phenotype of brain metastatic breast cancer cell clusters. BCBM cell spheroids attained a dormant phenotype when cultured on soft HA hydrogels, whereas they exhibited a size-dependent switch between the dormant and proliferative phenotypes on stiff HA hydrogels (i.e., Proliferative phenotype $\geq$ 5000 cells < Dormant phenotype). In addition, micro-colony formation was observed for 10k cells spheroid on stiff HA hydrogels. We also demonstrated that the stiffness induced dormancy was reversible. This system could provide a useful tool to investigate the signaling pathways involved in BCBM colonization by further incorporating various metastatic site specific cues (e.g., cellular cues) along with the mechanical cues investigated in this work. In addition, this system could also be utilized for screening anti-metastatic drugs.

Conflict of Interest

The authors declare that there are no conflicts of interest.

Acknowledgments

References

1. D. Hanahan and R. A. Weinberg, *Cell*, 2000, **100**, 57-70.

2. G. P. Gupta and J. Massagué, *Cell*, 2006, **127**, 679-695.

3. A. A. Narkhede, L. A. Shevde and S. S. Rao, *Int. J. Cancer*, 2017, **141**, 1091-1109.

4. K. L. Harper, M. S. Sosa, D. Entenberg, H. Hosseini, J. F. Cheung, R. Nobre, A. Avivar-Valderas, C. Nagi, N. Girnius, R. J. Davis, E. F. Farias, J. Condeelis, C. A. Klein and J. A. Aguirre-Ghiso, *Nature*, 2016, **540**, 588-592.

5. M. Giuliano, A. Shaikh, H. C. Lo, G. Arpino, S. De Placido, X. H. Zhang, M. Cristofanilli, R. Schiff and M. V. Trivedi, *Cancer Res.*, 2018, **78**, 845-852.

6. N. Aceto, A. Bardia, D. T. Miyamoto, M. C. Donaldson, B. S. Wittner, J. A. Spencer, M. Yu, A. Pely, A. Engstrom, H. Zhu, B. W. Brannigan, R. Kapur, S. L. Stott, T. Shioda, S. Ramaswamy, D. T. Ting, C. P. Lin, M. Toner, D. A. Haber and S. Maheswaran, *Cell*, 2014, **158**, 1110-1122.

7. K. J. Cheung, V. Padmanaban, V. Silvestri, K. Schipper, J. D. Cohen, A. N. Fairchild, M. A. Gorin, J. E. Verdone, K. J. Pienta, J. S. Bader and A. J. Ewald, *Proc. Natl. Acad. Sci. USA*, 2016, **113**, E854-863.

8. S. S. Rao, R. V. Kondapaneni and A. A. Narkhede, *J. Biol. Eng.*, 2019, **13**, 3-3.

9. S. Pradhan, J. L. Sperduto, C. J. Farino and J. H. Slater, *J. Biol. Eng.*, 2018, **12**, 37.

10. M. S. Sosa, P. Bragado and J. A. Aguirre-Ghiso, *Nat. Rev. Cancer*, 2014, **14**, 611-622.

11. S. Pradhan and J. H. Slater, *Biomaterials*, 2019, **215**, 119177.

12. A. A. Narkhede, J. H. Crenshaw, D. K. Crossman, L. A. Shevde and S. S. Rao, *Acta Biomater.*, 2020, DOI: 10.1016/j.actbio.2020.02.039.

13. N. Linde, G. Fluegen and J. A. Aguirre-Ghiso, *Adv. Cancer Res.*, 2016, **132**, 45-71.

14.   C. M. Ghajar, *Nat. Rev. Cancer*, 2015, **15**, 238-247.

15.   S.-Y. Park and J.-S. Nam, *Exp Mol Med*, 2020, DOI: 10.1038/s12276-020-0423-z.

16.   S. Paget, *Lancet*, 1889, **133**, 571-573.

17.   D. Barkan, J. E. Green and A. F. Chambers, *Eur J Cancer*, 2010, **46**, 1181-1188.

18.   J. Y. Lee and O. Chaudhuri, *ACS Biomater. Sci. Eng.*, 2018, **4**, 302-313.

19.   D. Barkan, H. Kleinman, J. L. Simmons, H. Asmussen, A. K. Kamaraju, M. J.
       Hoenorhoff, Z.-y. Liu, S. V. Costes, E. H. Cho, S. Lockett, C. Khanna, A. F. Chambers
       and J. E. Green, *Cancer Res.*, 2008, **68**, 6241-6250.

20.   D. Barkan and J. E. Green, *J Vis Exp*, 2011, DOI: 10.3791/2914, 2914.

21.   L. H. El Touny, A. Vieira, A. Mendoza, C. Khanna, M. J. Hoenerhoff and J. E. Green, *J
       Clin Invest*, 2014, **124**, 156-168.

22.   H. R. Lee, F. Leslie and S. M. Azarin, *J. Biol. Eng.*, 2018, **12**, 12.

23.   J. Y. Fang, S. J. Tan, Y. C. Wu, Z. Yang, B. X. Hoang and B. Han, *J Transl Med.*, 2016,
       14, 38.

24.   Y. Liu, J. Lv, X. Liang, X. Yin, L. Zhang, D. Chen, X. Jin, R. Fiskesund, K. Tang, J. Ma,
       H. Zhang, W. Dong, S. Mo, T. Zhang, F. Cheng, Y. Zhou, J. Xie, N. Wang and B.
       Huang, *Cancer Res.*, 2018, **78**, 3926-3937.

25.   Y. Kassim, E. Tawil, C. Buquet, D. Le Cerf and J. PierreVannier, *J Clin Exp Oncol.*,
       2017, **06**.

26.   J. Preciado, E. Reátegui, S. Azarin, E. Lou and A. Aksan, *Technology*, 2017, **05**, 1-10.

27.   J. Schrader, T. T. Gordon-Walker, R. L. Aucott, M. van Deemter, A. Quaas, S. Walsh, D.
       Benten, S. J. Forbes, R. G. Wells and J. P. Iredale, *Hepatology*, 2011, **53**, 1192-1205.

28. T. S. Pavan Grandhi, T. Potta, R. Nitiyanandan, I. Deshpande and K. Rege, *Biomaterials*, 2017, **142**, 171-185.

29. R. Marlow, G. Honeth, S. Lombardi, M. Cariati, S. Hessey, A. Pipili, V. Mariotti, B. Buchupalli, K. Foster, D. Bonnet, A. Grigoriadis, P. Rameshwar, A. Purushotham, A. Tutt and G. Dontu, *Cancer Res.*, 2013, **73**, 6886-6899.

30. D. M. Sosnoski, R. J. Norgard, C. D. Grove, S. J. Foster and A. M. Mastro, *Clin Exp Metastasis*, 2015, **32**, 335-344.

31. S. E. Wheeler, A. M. Clark, D. P. Taylor, C. L. Young, V. C. Pillai, D. B. Stolz, R. Venkataramanan, D. Lauffenburger, L. Griffith and A. Wells, *Br. J. Cancer*, 2014, **111**, 2342-2350.

32. A. S. Khazali, A. M. Clark and A. Wells, *Br. J. Cancer*, 2018, **118**, 566-576.

33. L. Jadin, S. Pastorino, R. Symons, N. Nomura, P. Jiang, T. Juarez, M. Makale and S. Kesari, *Ann Transl Med*, 2015, **3**, 80.

34. K. J. Wolf and S. Kumar, *ACS Biomater. Sci. Eng.*, 2019, **5**, 3753-3765.

35. B. Ananthanarayanan, Y. Kim and S. Kumar, *Biomaterials*, 2011, **32**, 7913-7923.

36. A. A. Narkhede, J. H. Crenshaw, R. M. Manning and S. S. Rao, *J. Biomed. Mater. Res. Part A*, 2018, **106**, 1832-1841.

37. A. Ivascu and M. Kubbies, *J. Biomol. Screen.*, 2006, **11**, 922-932.

38. P. S. Nakod, Y. Kim and S. S. Rao, *Biotechnol. and Bioeng.*, 2020, **117**, 511-522.

39. M. V. Monteiro, V. M. Gaspar, L. P. Ferreira and J. F. Mano, *Biomater. Sci.*, 2020, **8**, 1855-1864.

40. U. Grässer, M. Bubel, D. Sossong, M. Oberringer, T. Pohlemann and W. Metzger, *Ann Anat.*, 2018, **216**, 1-8.

41.   D. Barkan, L. H. El Touny, A. M. Michalowski, J. A. Smith, I. Chu, A. S. Davis, J. D. Webster, S. Hoover, R. M. Simpson, J. Gauldie and J. E. Green, *Cancer Res.*, 2010, **70**, 5706-5716.

42.   S. S. Rao, J. DeJesus, A. R. Short, J. J. Otero, A. Sarkar and J. O. Winter, *ACS Appl. Mater. Interfaces*, 2013, **5**, 9276-9284.

43.   Y. Jamin, J. K. R. Boult, J. Li, S. Popov, P. Garteiser, J. L. Ulloa, C. Cummings, G. Box, S. A. Eccles, C. Jones, J. C. Waterton, J. C. Bamber, R. Sinkus and S. P. Robinson, *Cancer Res.*, 2015, **75**, 1216-1224.

44.   A. N. May, B. D. Crawford and A. M. Nedelcu, *Front Oncol*, 2018, **8**.

45.   M. G. Ondeck, A. Kumar, J. K. Placone, C. M. Plunkett, B. F. Matte, K. C. Wong, L. Fattet, J. Yang and A. J. Engler, *Proc. Natl. Acad. Sci. USA*, 2019, **116**, 3502-3507.

46.   M. Sobecki, K. Mrouj, J. Colinge, F. Gerbe, P. Jay, L. Krasinska, V. Dulic and D. Fisher, *Cancer Res.*, 2017, **77**, 2722-2734.

47.   T. Scholzen and J. Gerdes, *J. Cell. Physiol.*, 2000, **182**, 311-322.

48.   A. Salic and T. J. Mitchison, *Proc. Natl. Acad. Sci. USA*, 2008, **105**, 2415.

49.   B. D. Lehmann, J. A. Bauer, X. Chen, M. E. Sanders, A. B. Chakravarthy, Y. Shyr and J. A. Pietenpol, *J Clin Invest*, 2011, **121**, 2750-2767.

50.   M. Singh, S. Mukundan, M. Jaramillo, S. Oesterreich and S. Sant, *Cancer Res.*, 2016, **76**, 3732-3743.

51.   M. Singh, H. Venkata Krishnan, S. Ranganathan, B. Kiesel, J. H. Beumer, S. Sreekumar and S. Sant, *ACS Biomater. Sci. Eng.*, 2018, **4**, 421-431.

52.   L. A. Kunz-Schughart, J. P. Freyer, F. Hofstaedter and R. Ebner, *J. Biomol. Screen.*, 2004, **9**, 273-285.

53.   K. Leone, C. Poggiana and R. Zamarchi, *Diagnostics (Basel)*, 2018, **8**, 59.

Figure legends:

Figure 1: Brain metastatic breast cancer cell spheroids exhibited differential growth responses over a period of 7 days depending on the culture condition and spheroid size. (a) Bright field and (b) florescent images (day 0) of cell spheroids prepared by using 100, 500, 1k, 2k, 5k and 10k MDA-MB-231Br cells (from left to right), Scale bar = 100μm. Area of cell spheroids in various culture conditions for (c) 100 cells spheroid (d) 500 cells spheroid (e) 1k cells spheroid (f) 2k cells spheroid (g) 5k cells spheroid (h) 10k cells spheroid over a period of 7 days. Blue – Suspension culture, Red – Stiff HA hydrogel (4.5kPa), Black – Soft HA hydrogel (0.4 kPa). N ≥ 5 replicates per each condition. ** indicates statistical significance ($p < 0.05$) compared to both soft and stiff HA hydrogel condition for area at day 7. * indicates statistical significance ($p < 0.05$) compared to soft HA hydrogel for area at day 7. Error bar represents standard error.

Figure 2: Stiffness and size-induced migration and formation of micro-colonies was observed in 10k cells spheroid when cultured on a stiff HA hydrogel (4.5 kPa) as opposed to culture on a soft HA hydrogel (0.4 kPa). (a) Day 1, (b) Day 7 bright field and florescent images of 10k cells spheroid cultured on a soft HA hydrogel. (c) Day 1, (d) Day 7 bright field and florescent images of 10k cells spheroid cultured on a stiff HA hydrogel and (e) Distance of micro-colonies from the spheroid periphery. N ≥ 8 replicates per each condition.
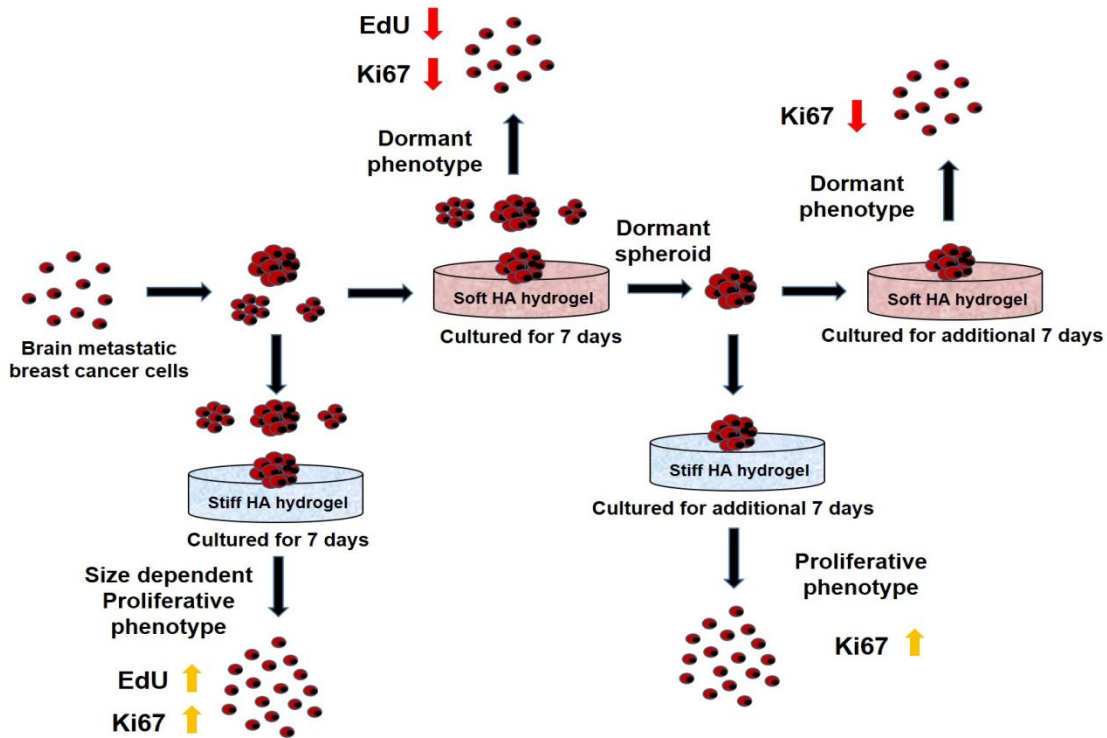
Figure 3: Brain metastatic breast cancer cells in 10k spheroid cultured on soft HA hydrogel (0.4 kPa) were Ki67 negative and displayed a dormant phenotype compared to stiff HA hydrogel (4.5 kPa). (a) Representative fluorescent images of Ki67 staining for MDA-MB-231Br cells obtained from 10k spheroid cultured in various culture conditions. Blue – DAPI (nucleus), Green – Ki67, Scale bar =100 μm. (b) Quantification of Ki67 positive cells in 10k spheroid cultured on soft or stiff HA hydrogel, suspension, and adherent cultures respectively. N ≥ 4 replicates per condition.

**indicates statistically significant difference ($p < 0.05$) compared to soft and stiff HA hydrogel and suspension culture. * indicates statistically significant difference ($p < 0.05$) compared to soft HA hydrogel. Error bar indicates standard error.

Figure 4: Stiffness induced dormant phenotype observed on the soft HA hydrogel (0.4 kPa) for 10k cells spheroid was reversible. (a) Schematic depicting the transfer of 10k cells spheroid from soft HA hydrogel to another soft or stiff HA hydrogel. (b) Day 7 bright field and fluorescent images of 10k cells spheroid cultured on soft HA hydrogel and Day 14 bright field and fluorescent images of 10k cells spheroid transferred from soft HA hydrogel on day 7 to soft or stiff HA hydrogel and cultured for an additional 7 days. Scale bar = 200 μm. (c) Area of 10k cells spheroid measured over a period of 14 days. N ≥ 6 replicated per each condition. * indicates statistical significance (p < 0.05) compared to the 'soft to soft' condition for area at day 14. Error bar represents standard error.

Figure 5: Brain metastatic breast cancer cells in 10k cells spheroid expressed a higher percentage of Ki67 positivity at day 14 when transferred from soft HA hydrogel (0.4 kPa) to stiff HA hydrogel (4.5 kPa) as compared to those transferred from soft to soft HA hydrogels. (a) Representative fluorescent images of Ki67 staining for MDA-MB-231Br cells in 10k cells spheroid cultured on soft HA hydrogel for 7 days and transferred to soft or stiff HA hydrogel and cultured for an additional 7 days, Blue – DAPI (nucleus), Green – Ki67, (b) Quantification of Ki67 positive cells present in 10k cells spheroid on soft or stiff HA hydrogel post transfer. N = 4 replicates per condition. * indicates statistically significant difference ($p < 0.05$) compared to the 'soft to soft' condition. Error bar indicates standard error.

Table of Contents Entry:

Dormant versus proliferative phenotype in metastatic tumor cell clusters is mediated via matrix stiffness and cluster size
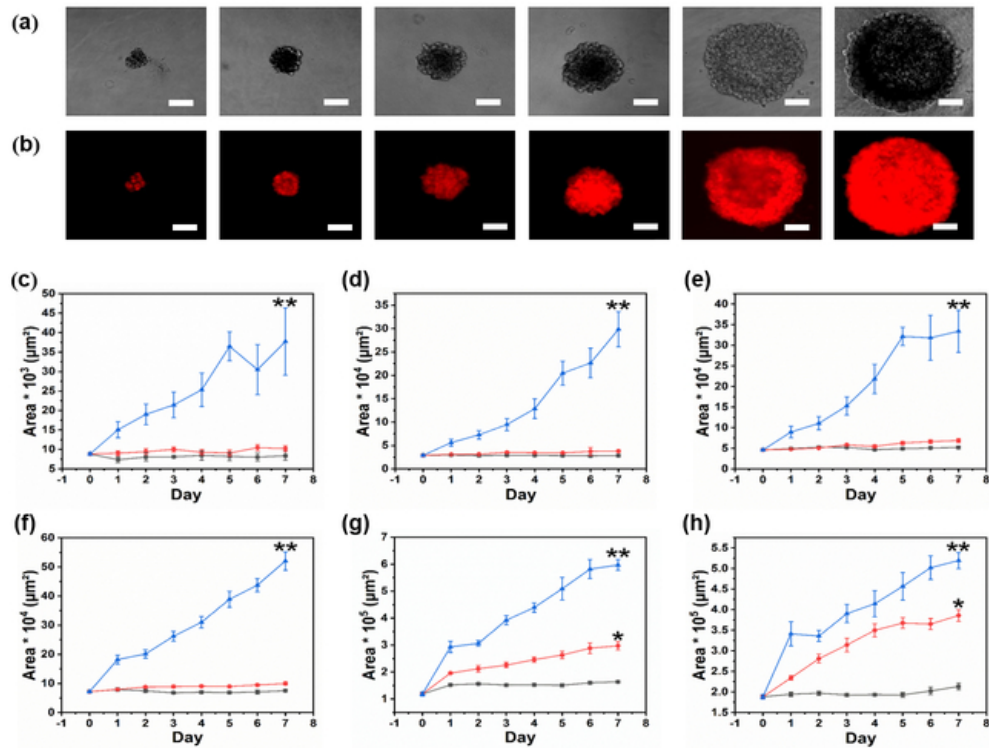
Figure 1: Brain metastatic breast cancer cell spheroids exhibited differential growth responses over a period of 7 days depending on the culture condition and spheroid size. (a) Bright field and (b) florescent images (day 0) of cell spheroids prepared by using 100, 500, 1k, 2k, 5k and 10k MDA-MB-231Br cells (from left to right), Scale bar = 100µm. Area of cell spheroids in various culture conditions for (c) 100 cells spheroid (d) 500 cells spheroid (e) 1k cells spheroid (f) 2k cells spheroid (g) 5k cells spheroid (h) 10k cells spheroid over a period of 7 days. Blue – Suspension culture, Red – Stiff HA hydrogel (4.5kPa), Black – Soft HA hydrogel (0.4 kPa). N ≥ 5 replicates per each condition. ** indicates statistical significance ($p < 0.05$) compared to both soft and stiff HA hydrogel condition for area at day 7. * indicates statistical significance ($p < 0.05$) compared to soft HA hydrogel for area at day 7. Error bar represents standard error.
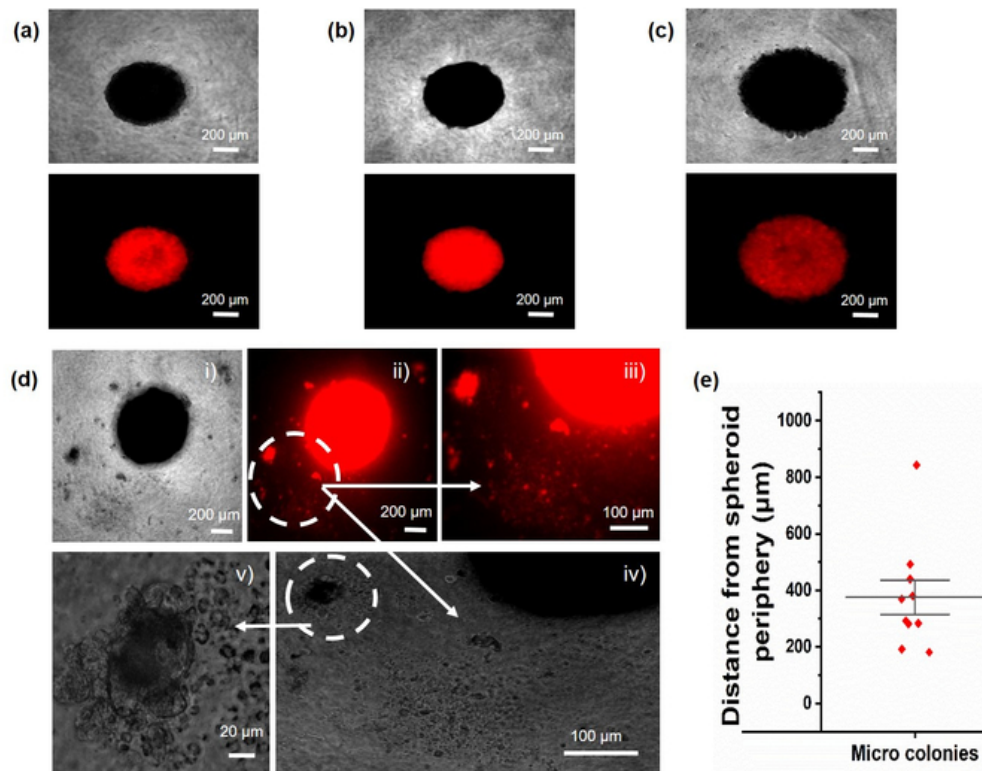
55x41mm (300 x 300 DPI)

Figure 2: Stiffness and size-induced migration and formation of micro-colonies was observed in 10k cells spheroid when cultured on a stiff HA hydrogel (4.5 kPa) as opposed to culture on a soft HA hydrogel (0.4 kPa). (a) Day 1, (b) Day 7 bright field and florescent images of 10k cells spheroid cultured on a soft HA hydrogel. (c) Day 1, (d) Day 7 bright field and florescent images of 10k cells spheroid cultured on a stiff HA hydrogel and (e) Distance of micro-colonies from the spheroid periphery. N ≥ 8 replicates per each condition.
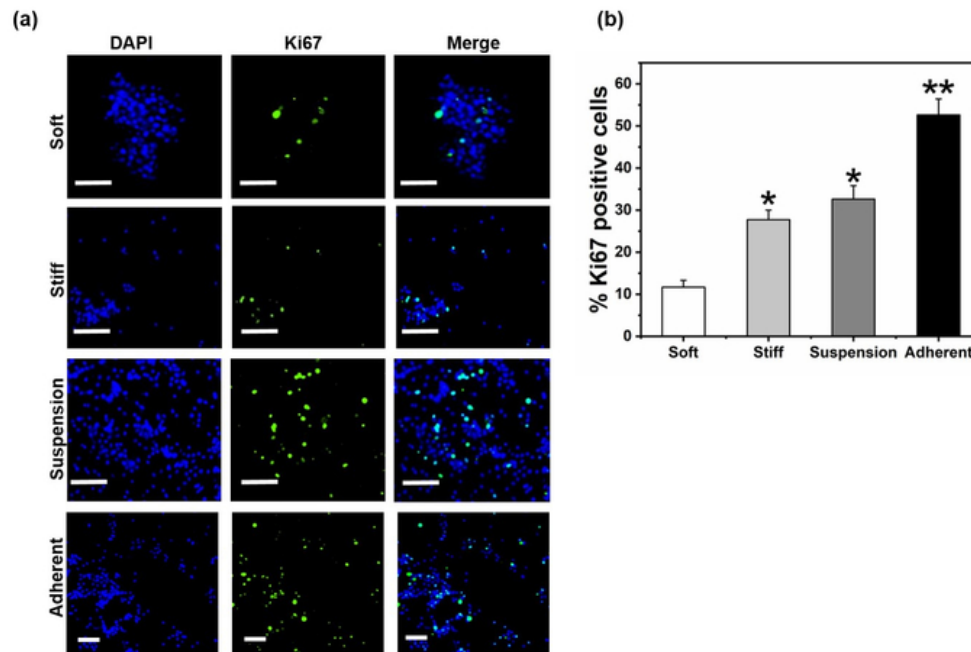
56x43mm (300 x 300 DPI)

Figure 3: Brain metastatic breast cancer cells in 10k spheroid cultured on soft HA hydrogel (0.4 kPa) were Ki67 negative and displayed a dormant phenotype compared to stiff HA hydrogel (4.5 kPa). (a) Representative fluorescent images of Ki67 staining for MDA-MB-231Br cells obtained from 10k spheroid cultured in various culture conditions. Blue – DAPI (nucleus), Green – Ki67, Scale bar =100 µm. (b) Quantification of Ki67 positive cells in 10k spheroid cultured on soft or stiff HA hydrogel, suspension, and adherent cultures respectively. N ≥ 4 replicates per condition. **indicates statistically significant difference ($p < 0.05$) compared to soft and stiff HA hydrogel and suspension culture. * indicates statistically significant difference ($p < 0.05$) compared to soft HA hydrogel. Error bar indicates standard error.
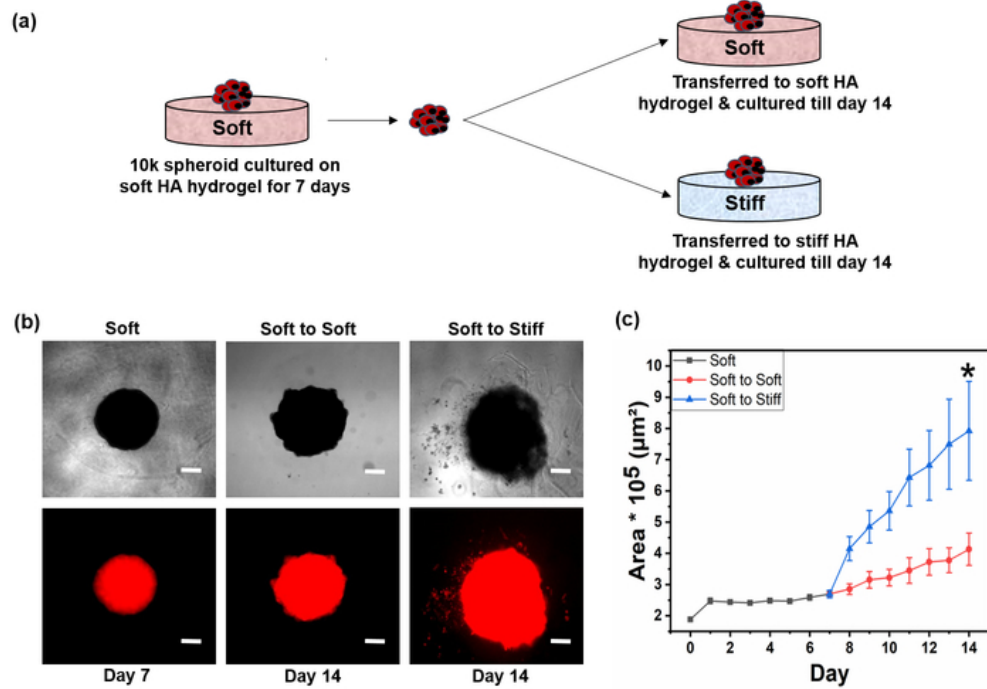
58x38mm (300 x 300 DPI)

Figure 4: Stiffness induced dormant phenotype observed on the soft HA hydrogel (0.4 kPa) for 10k cells spheroid was reversible. (a) Schematic depicting the transfer of 10k cells spheroid from soft HA hydrogel to another soft or stiff HA hydrogel. (b) Day 7 bright field and fluorescent images of 10k cells spheroid cultured on soft HA hydrogel and Day 14 bright field and fluorescent images of 10k cells spheroid transferred from soft HA hydrogel on day 7 to soft or stiff HA hydrogel and cultured for an additional 7 days. Scale bar = 200 µm. (c) Area of 10k cells spheroid measured over a period of 14 days. N ≥ 6 replicated per each condition. * indicates statistical significance ($p < 0.05$) compared to the 'soft to soft' condition for area at day 14. Error bar represents standard error.
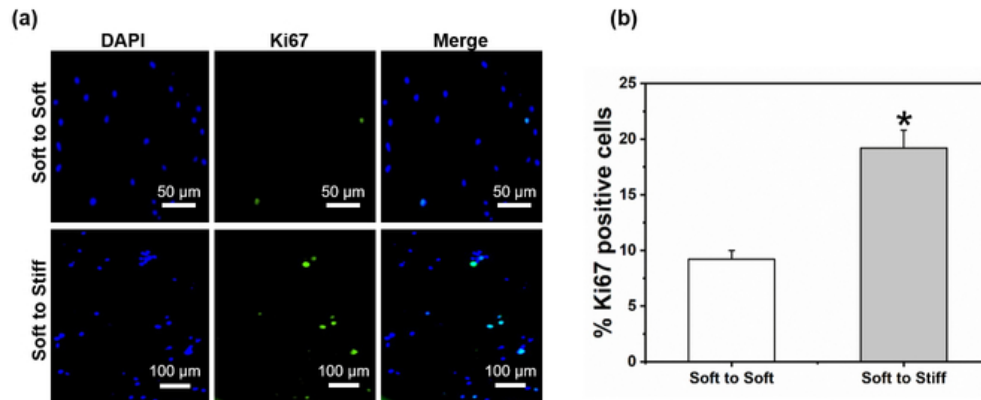
59x41mm (300 x 300 DPI)

Figure 5: Brain metastatic breast cancer cells in 10k cells spheroid expressed a higher percentage of Ki67 positivity at day 14 when transferred from soft HA hydrogel (0.4 kPa) to stiff HA hydrogel (4.5 kPa) as compared to those transferred from soft to soft HA hydrogels. (a) Representative fluorescent images of Ki67 staining for MDA-MB-231Br cells in 10k cells spheroid cultured on soft HA hydrogel for 7 days and transferred to soft or stiff HA hydrogel and cultured for an additional 7 days, Blue – DAPI (nucleus), Green – Ki67, (b) Quantification of Ki67 positive cells present in 10k cells spheroid on soft or stiff HA hydrogel post transfer. N = 4 replicates per condition. * indicates statistically significant difference ($p < 0.05$) compared to the 'soft to soft' condition. Error bar indicates standard error.

56x22mm (300 x 300 DPI)